ELSEVIER

Contents lists available at ScienceDirect

Materials Today Communications

journal homepage: www.elsevier.com/locate/mtcomm



Influence of a biaxially corrugated core geometry on flexural stiffness of wood-strand composite sandwich panels



Mostafa Mohammadabadi^a, Vikram Yadama^{b,*}

- ^a Material Science and Engineering Program and Composite Materials and Engineering Center, Washington State University, Pullman, WA 99164, USA
- b Department of Civil and Environmental Engineering and Composite Materials and Engineering Center, Washington State University, Pullman, WA 99164, USA

ARTICLE INFO

Keywords:
Parametric study
Biaxially corrugated core
Finite element model
Wood-strand composite
Sandwich panel

ABSTRACT

The objective of this study is to gain an understanding of the influence of a biaxially corrugated core geometry on flexure stiffness of wood-strand composite sandwich panel for building construction applications where member deflections often govern the design. To this aim, a parametric study was conducted using a finite element (FE) model to understand the sensitivity of the bending stiffness of a wood strand composite core to all variations in its geometry. A unit cell (UC) in the core was defined to simplify the determination of all parameters capable of altering the core geometry. Although eight parameters were chosen for this parametric study, the interaction between these parameters in changing the geometry required simulation of 13 cases to fully understand the influence of these eight core parameters on the bending stiffness. The comparison between the bending stiffness normalized by the width of the test specimens not only indicated the effect of these parameters on the bending stiffness but also revealed the effectiveness of each parameter. Based on these results, the geometry of the core was redesigned to increase the flexural stiffness. The bending stiffness of the new and redesigned core was 43 % and 126 % stiffer than the initial core in the longitudinal and transverse directions, respectively. After manufacturing a new mold based on these result and fabrication of a wood strand core, the experimental results exceeded our expectation. The experimental results revealed that the bending stiffness of the new core is 59 % and 203 % higher than initial one in the longitudinal and transverse directions, respectively.

1. Introduction

Sandwich panels have been extensively employed in aerospace, automotive, and civil industries due to high performance and high stiffness to weight ratio. As a classification, the core can be a continuous geometry such as metallic foam or a discrete one with periodic geometry such as honeycomb and corrugated cores [1]. Although discrete cores have higher performance compared to continuous ones, their high-cost manufacturing process could be an issue [2]. To address this issue and some environmental concerns, the purpose of this study is designing a high performance biaxially corrugated core that is fabricated from underutilized timber.

Use of renewable feedstock, such as wood strands offer more environmentally friendly options, especially if they originate from low-value feedstock, such as small diameter and fast-growing trees, to produce high-performance wood composite materials [3,4]. Oriented strand board (OSB), plywood, and structural composite lumbers (SCL) (e.g., parallel strand lumber (PSL); oriented strand lumber (OSL); and laminated strand lumber (LSL)) are examples of the wood-based

composite materials that are solid panels produced from lower quality wood for use as building construction materials. Compared to these solid panels of the same mass, sandwich panels produced from wood strands provide significantly higher stiffness and strength and use far less materials, fiber and resin. Additionally, sandwich panels with three-dimensional (3D) cores introduce cavities that can be filled with insulation to improve energy efficiency of building envelopes. Structural insulated panels (SIPs) are sandwich panels with thick insulated foam core and OSB outer layers developed for building construction applications and offer products with greater strength- and stiffness-toweight ratio [5,6]. However gravity load carrying capacity of these sandwich panels is an issue. Wood-based sandwich panels with corrugated cores are another option for building construction [7-9]. These types of sandwich structures are ideally suited for developing prefabricated building envelopes that are energy efficient and structurally sound. One such product is a recently developed wood-strand composite sandwich panel with a biaxially corrugated core for structural applications (Fig. 1) [10]. Research has shown that this sandwich panel demonstrates higher bending stiffness and performance than typical

^{*} Corresponding author.

E-mail address: vyadama@wsu.edu (V. Yadama).



Fig. 1. Wood composite sandwich panel configuration; biaxial corrugated ore and flat panels.

sheathing materials such as plywood and OSB [11–13]. Therefore, further improving the performance of the 3D wood-strand core sandwich panels would enable them to be introduced into the engineering and construction marketplaces not only as a sheathing material but also as a replacement for traditional building envelope materials through development of prefabricated panelized components (e.g., wall or floor systems).

Parametric analysis is commonly conducted to assess the influence of input factors on the output of interest. Using FE analysis, a parametric study was performed to examine the effect of changes in geometry, loading, and material properties on the buckling load of corrugated core sandwich panels made of paper sheet [14]. The collapse load was found to be very sensitive to changes in the core thickness. A 3D numerical model with Abaqus software was developed to conduct a parametric study in order to understand the effect of wall thickness and filling modes on the blast resistance of a honeycomb sandwich structure filled with circular tubes [15].

A Finite element approach was used to optimize the shape of the composite corrugated panel by minimizing the in-plane stiffness and maximizing flexural out of plane stiffness [16]. The bending performance of a double circular tubes filled with structural epoxy foam Terocore® subjected to quasi-static and dynamic loads was investigated using experiment and FE analyses [17]. The FE model developed with LS-DYNA was utilized to perform a parametric study to reveal the effect of individual components of the hybrid structure on the overall EA. Two FE models, 2D and 3D, were employed to study the influence of parameters such as rib angle, rib thickness, and pattern width on the structural performance of a 3D engineered fiberboard ply [18].

For structural panel used as wall sheathing, higher stiffness allows it to resist shear forces; and used as roof or floor sheathing, higher stiffness offers more resistance to deflection under uniform and concentrated loads. The objective of this study was to design a new corrugated geometry with higher performance. As the fabrication process and materials, such as strands and resin, were not going to be changed, only the influence of geometric parameters of the core ply was considered to design a corrugated panel with greater bending stiffness. However, the FE model can be used to explore the effect of using different materials, such as carbon or glass fibers, on the bending stiffness.

In this study, a parametric study was performed while considering interrelationships between different sets of geometric variables to understand the effect of the complicated geometry of a biaxially

corrugated core on its bending stiffness. This study is unique as it provides an approach to understand the interdependency of the variables that describe the core geometry, and ways to capture their influence on the bending stiffness of a sandwich panel with a complex core geometry. To this end, influence of eight parameters that were capable of changing the core geometry was evaluated and understood. This parametric study revealed the effect of these core parameters on the bending stiffness, and also the effectiveness of each parameter compared to the others. Based on the results from the parametric study and knowledge of the hot-pressing process [19], the core geometry was redesigned to obtain a higher bending stiffness and to meet the limitations of the manufacturing process. The new mold to manufacture redesigned wood-strand 3D core was fabricated. The experimental results of the redesigned core were used to verify the design process (a flowchart describing this process is presented in Fig. 2).

2. Material and methods

A corrugated panel (Fig. 1) was fabricated by hot pressing ponderosa pine (Pinus ponderosa) wood strands that were resinated with phenol formaldehyde. Thin wood strands with an average length of 152 mm, width of 199 mm, and thickness of 0.36 mm were produced using a CAE disk-strander operating at a rotational speed of 500 rpm. Wood strands were dried to a target moisture content of 3-5 % and sprayed with aerosolized liquid phenol formaldehyde (PF) resin (Hexion Specialty Chemicals, Springfield, OR, USA) in a drum blender to a target resin solid content of 8 % of the oven-dry wood weight; no other additive, such as wax, was added. Properties of the PF resin specified by the company are refractive index of 1.4944, percent solids of 57.45, percent alkalinity of 3.03, Brookfield viscosity @ 25 °C of 156 cps, pH between 9.2 and 11.2, boiling point of 102 °C, and relative density of 1.195 to 1.258. Subsequently, the resinated wood strands were oriented and hand-formed unidirectionally to form a mat of wood strands or preform. To manufacture the outer flat plies and the corrugated core panels using a matched-die mold, the unidirectional mat was consolidated and hot-pressed to a target thickness of 6.35 mm for 6 min at 160 °C. To fabricate the sandwich panels, flat panels were bonded with a two-part epoxy resin (Loctite epoxy by Henkel) to the biaxial corrugated cores with a uniform pressure between 50 and 75 psi. Sandwich panels were kept in a conditioning room to reach 10 %–12 %moisture content prior to testing. Mechanical behavior, such as impact [11], internal bond (IB) [12], and creep [13] along with analytical model [20] of the sandwich panel have been evaluated and published.

As the objective of the study was to redesign a new core with significantly higher bending stiffness, deformation within the elastic region was considered in this study. To have a better and reasonable comparison between the bending results of the sandwich panel and its core, and also to explore the contribution of the core to the bending stiffness of the sandwich panel, same dimensions were chosen for the sandwich panel and 3D Core layer specimens based on ASTM D7249 [21]. Abaqus finite element software was used to analyze the bending behavior of the sandwich panel and 3D core layer. The flat outer layers

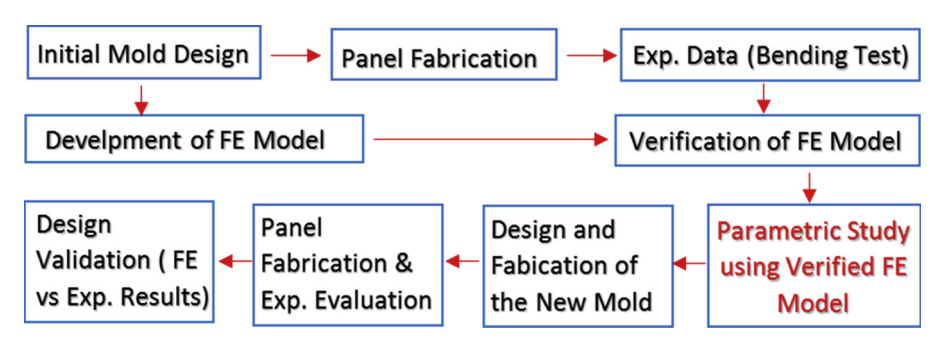


Fig. 2. A flowchart depicting the scope of the study and the design process (the highlighted box is the focus of this paper).

 Table 1

 Material properties of the wood-strand composite.

E ₁ (GPa)	E ₂ (GPa)	E ₃ (GPa)	ν_{12}	ν_{13}	$ u_{23}$	G ₁₂ (GPa)	G ₁₃ (GPa)	G ₂₃ (GPa)
9.80	1.71	1.71	0.358	0.358	0.2	2.56	2.56	0.71

were modeled using solid elements (C3D8R), while shell elements (S4R) were used to model the 3D core because of having a complex geometry. Use of shell elements for the core layer significantly decreases the simulation time and running time of the FE model. Since the thickness of the core layer is not modeled for the shell elements, fine mesh can also be adopted to have more accurate results. In addition, the ability of shell elements to undergo large strains as well as their suitability for both thin and thick shells is another reasoning to choose them for the core layer [22].

Since all wood strands were aligned in the same direction (\pm 35° with respect to the x-axis) to fabricate the outer and the core layers, transverse isotropy was assumed to define the material properties of both layers [23]. The required material properties to model the sandwich panel and its components are summarized in Table 1. Tie constraint was used to simulate the assumption of perfect bonding between the 3D core and the face sheets. Since the FE simulation must be consistent with the experimental test, nodes in the contact area between the specimens with supports were constrained in the Z-direction to apply boundary conditions. Following ASTM D7249 [21], both 3D core and sandwich panel specimens were submitted to 4-point bending test. The load-deflection curve obtained from the flexure test was used to calculate the bending stiffness as

$$D = \frac{Pa}{24\Delta} (3L^2 - 4a^2) \stackrel{a = \frac{L}{3}, m = \frac{P}{\Delta}}{\to} D = \frac{23mL^3}{1296}$$
 (1)

Where P, Δ , L, and m are bending load, deflection at mid-span, span length, and slope of the load-deflection curve, respectively. The constant "a" is the distance between the support and loading point.

The bending test results of the sandwich panel and the 3D core show a strong agreement between the FE model and experimental test in the elastic region (Fig. 3). In case of the core, the difference between FE and the experimental results in the transverse and longitudinal directions were 0.3 % and 1.4 %. As for the sandwich panel, the difference between FE and the experimental results in transverse and longitudinal directions were 7.3 % and 5.6 %. Subsequent to verification of the FE model, it was employed to conduct a parametric study to redesign the core geometry to yield a sandwich panel with significantly increased flexure stiffness.

3. Core parameters and required cases

In order to understand the effect of the geometry of the core on its bending stiffness, the first step is to identify and determine the core geometric parameters that are influential and can be modified.

Therefore, a unit cell (UC) was defined as the simplest repeating element in both the longitudinal and transverse directions of the 3D core (Fig. 4).

Since any change in the core geometry stems from modification in this UC configuration, all parameters that are capable of manipulating the UC configuration were considered as core geometric parameters (shown in Fig. 4b). These parameters were categorized in three groups in accordance with their directions shown in Fig. 4a: 1- longitudinal parameters (L_1 , X_1 , and θ_1), 2- transverse parameters (L_2 , Y_{21} , and Y_{22}), and 3- normal parameters (h and h). Note that parameters h1, h2, and h3, h3 are dimensions that describe the interfacial bonding area between the core and the face plies of a sandwich panel.

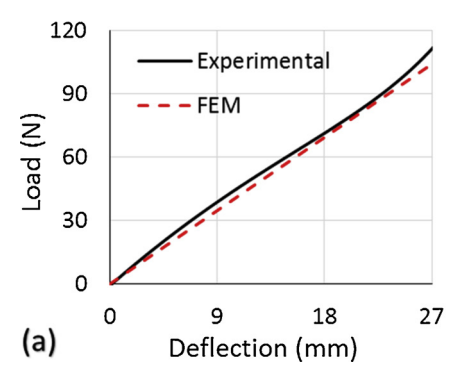
Finite element analysis conducted on a 3D fiberboard core by Hunt [18] revealed that the minimum deformation due to bending and flatwise compression tests are achieved when the major rib angle, θ_2 , has a value between 50° and 60°. Therefore, in this study, θ_2 was maintained at 56° [10].

Due to interdependency between the core parameters, it is impossible to change one parameter without the other parameters changing. Therefore, to modify any longitudinal or transverse parameter, another longitudinal or transverse parameter must be modified simultaneously. For example, in Fig. 5a and b, a change in transverse UC length (L_2) must also modify transverse bonding length 1 (Y_{21}) as in Case 7 or transverse bonding length 2 (Y_{22}) as in Case 5. However, to add to the complexity of this analysis, modification of a normal parameter in the z-axis, h or t, requires changes in two parameters, one in the longitudinal and one in the transverse direction. For example, amplitude, h, can be increased or decreased by changing longitudinal UC length (L_1) and transverse UC length (L_2) as in Case 1 or by changing minor rib angle (θ_1) and transverse UC length (L_2) as in Case 2 (Fig. 5c and d).

The interaction between the eight UC geometric parameters (not including θ_2) requires an analysis of 13 cases to understand the influence of each parameter on the bending stiffness of the core. A summary of all these cases with the corresponding changing parameters is provided in Table 2.

4. Results and discussion

For each of the 13 cases in Table 2, at least four different UCs were generated by modifying the corresponding parameters. Subsequently, UC was duplicated in the longitudinal and transverse directions to create a 3D core. From a four-point bending test on both the longitudinal and transverse specimens cut from the 3D core, load-deflection



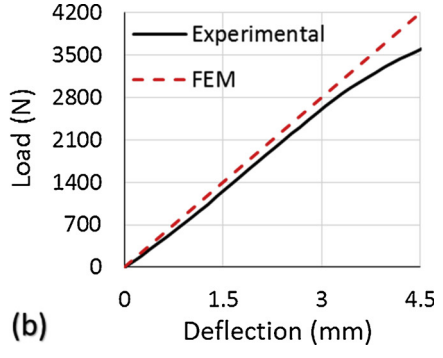


Fig. 3. Load- deflection curves from a 4-point bending test of (a) a 3D core layer in transverse, and (b) a sandwich panel in longitudinal directions.

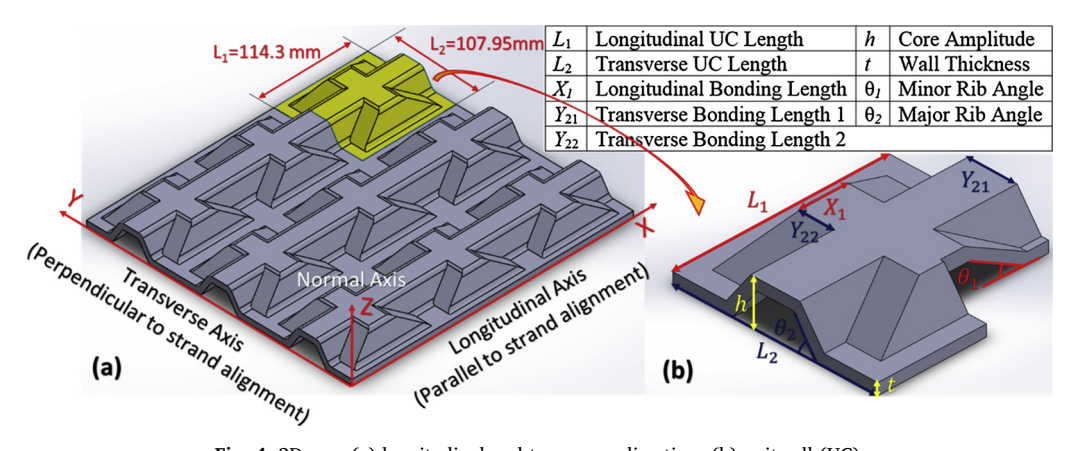


Fig. 4. 3D core (a) longitudinal and transverse directions (b) unit cell (UC).

curves were obtained to calculate the longitudinal and transverse bending stiffness (Eq. (1)). As mentioned earlier, a span length of 559 mm was chosen for both the longitudinal and transverse specimens of sandwich panels and 3D core layers based on ASTM D7249 [21]. This procedure was repeated for all UCs and all cases. For better comparison among all the cases, the bending stiffness value of each specimen was normalized by the width of that specimen.

4.1. Evaluation of amplitude (h)

Core amplitude can be varied by changing different sets of core geometric parameters. To understand the effect of change in core amplitude on its bending stiffness, four different cases as shown in Table 3 were investigated, where in each case a pair of geometric parameters were varied to change the amplitude. The normalized core bending stiffness in the longitudinal and transverse directions for these four cases are reported in Figs. 6 and 8 respectively. To differentiate the cases, the results of each case are connected by dotted lines; these dotted lines do not imply any trend between the bending stiffness and the corresponding variable.

Except in the fourth longitudinal specimen of the case 1 shown in Fig. 6, increase in amplitude indicates a rising trend in the normalized bending stiffness of the longitudinal specimen. This trend, despite having the largest amplitude, can be explained by examining the second moment of area for one UC in the longitudinal direction (Fig. 7a). The slanted sections of the core (2 and 4) have a lower moment of inertia than the horizontal Sections (1, 3, and 5). Since these slanted sections or walls are larger and more dominant than other sections in the fourth longitudinal specimen configuration (No 4 of Case 1 in Fig. 6), the average bending stiffness is reduced. Another reason for this decrease in bending stiffness is due to the instability caused by larger amplitude.

As for Case 2, any increase in the changing parameters leads to an increase in the normalized bending stiffness of both longitudinal and transverse directions (Figs. 6 and 8). Since the only difference between these two cases is replacing the longitudinal UC length (L_1) in the first case with the minor rib angle (θ_1) in the second case (Table 3), it shows that any increase in minor rib angle has a positive effect on the longitudinal bending stiffness compared to longitudinal UC length. In addition, unlike in case 1, large amplitude does not give rise to reduction in the longitudinal bending stiffness of the second case (Fig. 6). In fact,

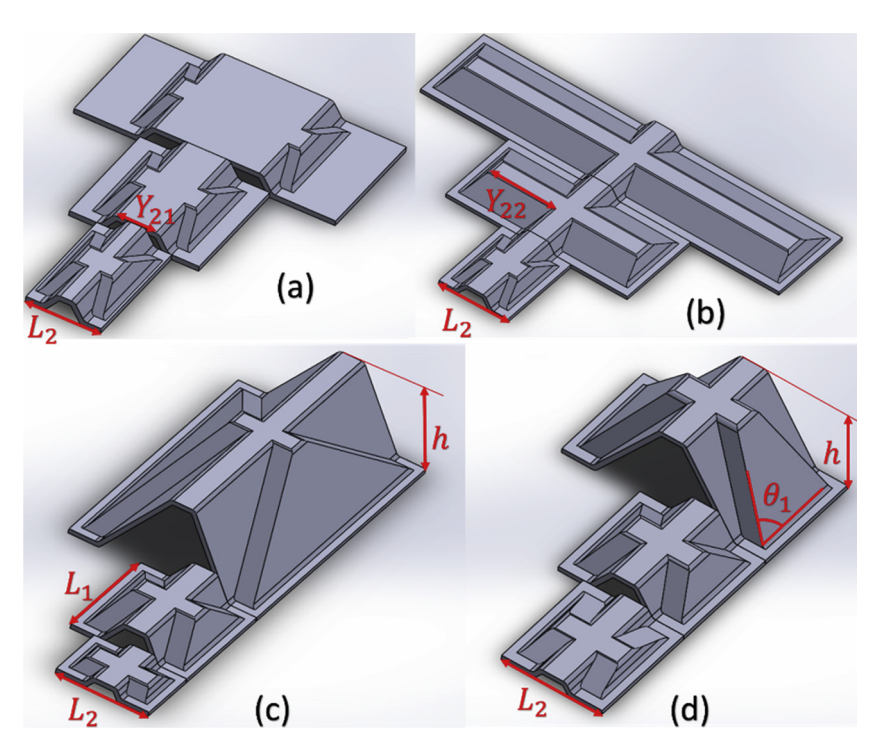


Fig. 5. Interrelationship between transverse UC length, L_2 , and (a) transverse bonding length 1, Y_{21} (Case 7) (b) transverse bonding length 2, Y_{22} (Case 5), and Interrelationship between L_2 and (a) L_1 and h (Case 1) (b) θ 1 and h (Case 2).

Table 2Interrelated geometric parameters varied in each of the 13 cases analyzed to redesign the core geometry.

Case	Changing parameters	Case	Changing parameters	Case	Changing parameters	Case	Changing parameters	Case	Changing parameters
1	h, L ₁ , L ₂	2	h, θ_1 , L_2	3	h, L ₁ , Y ₂₂	4	h, θ_1 , Y_{22}	5	L ₂ , Y ₂₂
6	L_2, Y_{21}, Y_{22}	7	L_2, Y_{21}	8	L_1, θ_1	9	θ_1, X_1	10	L_1, X_1
11	t, L_1, L_2	12	t, h, Y ₂₂	13	t, X ₁ , Y ₂₂				

Table 3
Corresponding cases and core parameters to evaluate h.

Case	Constant Parameters (mm)	Changing Parameters		Dimension of changing parameters for each UC (mm)			
			First UC	Second UC	Third UC	Fourth UC	
1	$\theta_1 = 30^\circ, t = 6.35$	h	17.78	25.4	40.64	111.76	
	$X_1 = Y_{21} =$	L_1	93.80	120.2	172.99	419.35	
	$Y_{22} = 25.4$	L_2	123.77	134.05	154.61	250.55	
2	$L_1 = 139.7,$	h	17.78	25.4	40.64	111.76	
	t = 6.35,	θ_1	14.68°	23.848°	39.1°	69.19°	
	$X_1 = Y_{21} =$	L_2	123.77	134.05	154.61	250.55	
	$Y_{22} = 25.4$						
3	$L_2 = 139.7,$	h	17.78	22.86	30.48	43.18	
	$\theta_1 = 30^{\circ}, t = 6.35,$	L_1	93.80	111.39	137.79	181.79	
	$X_1 = Y_{21} = 25.4$	Y_{22}	33.36	29.94	24.8	16.23	
4	$L_1 = L_2 = 139.7,$	h	17.78	22.86	30.48	43.18	
	t = 6.35,	θ_1	14.68°	20.88°	29.42°	41.21°	
	$X_1 = Y_{21} = 25.4$	Y_{22}	33.36	29.94	24.8	16.23	

the shrinkage of the inclined Sections (2 and 4 in Fig. 7a) and the presence of more horizontal Sections (1,3, and 5 in Fig. 7a) in the fourth longitudinal specimen of the second case prevent reduction in the moment of inertia. Based on the results of the first two cases, amplitude is an influential parameter to improve the bending stiffness.

In Case 3, an increase in amplitude of the UC leads to a decrease in transverse bonding length 2 (Y_{22}) , thus the normalized transverse bending stiffness decreases significantly for amplitude of over 25 mm (Fig. 8). As amplitude is increased, however, the bonding length 2 (Y_{22}) decreases and results in a reduction of the transverse bending stiffness; these two parameters (amplitude and transverse bonding length 2)

compete to affect the transverse bending stiffness. Reduction of transverse bending stiffness (Case 3 in Fig. 8) shows how this stiffness is more sensitive to a reduction in transverse bonding length 2 than an increase in amplitude.

Sensitivity of transverse bending stiffness to transverse bonding length 2 (Y_{22}) can be explained by computing the second moment of area for one UC in the transverse direction (Fig. 7b). Unlike the moment of inertia in the longitudinal direction (Fig. 7a), inclined Sections (2 and 4) have a higher moment of inertia than horizontal Sections (1, 3, and 5). Therefore, reduced transverse bonding length 2 (Y_{22}) leads to a decrease in the second moment of area which results in a drop in the transverse bending stiffness.

Change in amplitude increases the longitudinal bending stiffness as demonstrated in Case 4 (Fig. 6). Similar to Case 3, transverse bonding length 2 has the opposite effect from that of amplitude on the transverse bending stiffness in Case 4 (Fig. 8). Amplitude is initially more dominant than transverse bonding length 2 in influencing the transverse bending stiffness such that an increase in this parameter leads to an increase in the bending stiffness even though transverse bonding length 2 is decreased. However, a decrease in transverse bonding length 2 beyond a critical point, which could vary from case to case, significantly reduces the transverse bending stiffness.

4.2. Evaluation of transverse bonding lengths (Y_{21} and Y_{22})

Transverse bonding lengths (Y_{21} and Y_{22}) are important parameters because they alter the core geometry and determine the bonding surface area between the core and outer layers. Small bonding surface area results in sandwich panel with low shear strength between the core and face sheets. Therefore, three cases as shown in Table 4 are investigated

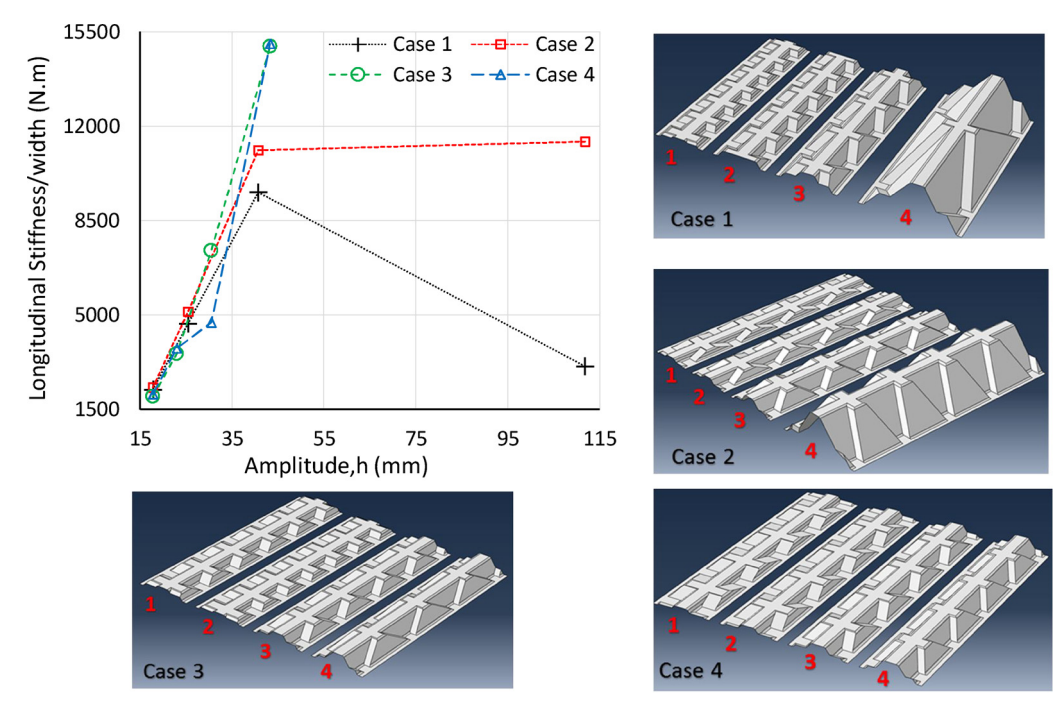


Fig. 6. Normalized bending stiffness and corresponding specimens for case 1-4 in longitudinal direction.

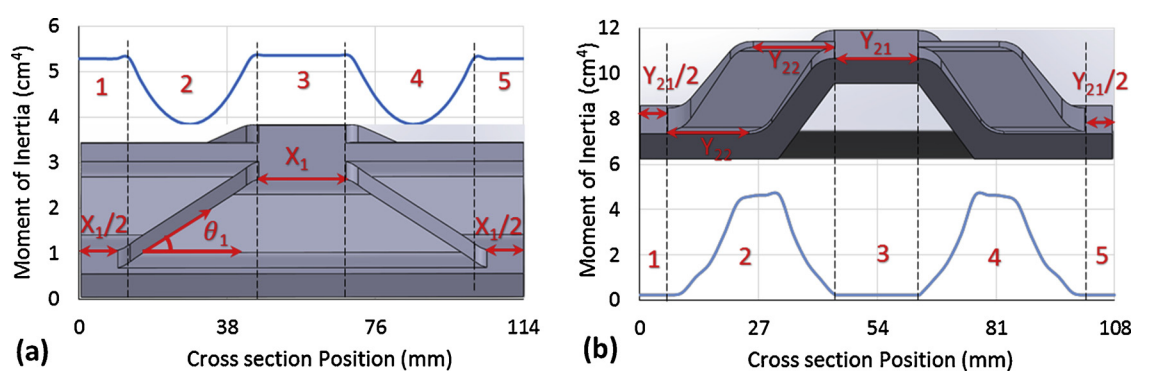


Fig. 7. Variation in the second moment of area for one UC in the (a) longitudinal and (b) transverse direction.

to examine the effect of changes in these parameters on the bending stiffness of the core.

Although Case 3 indicates that reduction in transverse bonding length 2 (Y_{22}) decreases the transverse bending stiffness, its effect on the longitudinal bending stiffness was not evaluated. Therefore, this parameter (Y_{22}) were chosen as varying parameters in Case 5 and 6.

Any increase in Y_{22} has a negative effect on the longitudinal bending stiffness as shown in Fig. 9. When the core is subjected to flexure loads, the deformed shape has two curvatures - a dominant or primary one in the longitudinal direction and a secondary one in the transverse direction due to localized bending of the unit cells about the other principal axis. Due to this transverse curvature, an increase in width of the unit cell will lead to a reduction of longitudinal bending stiffness. An increase in Y_{22} significantly increases transvers bending stiffness (Fig. 10). Increased transverse bonding length 2 (Y_{22}) results in expansion of the inclined Sections (2 and 4 shown in Fig. 7b), which increases the second moment of area and transverse bending stiffness.

In Case 7, the effect of change in transverse bonding length 1 (Y_{21}) was investigated while transverse bonding length 2 (Y_{22}) was held constant (Fig. 11). Initially, an increase in transverse bonding length 1 (Y_{21}) improves the longitudinal bending stiffness as a consequence of an increase in the moment of inertia; however the longitudinal bending stiffness reduces with wider specimens due to transverse curvature that

results in additional deflection in the transverse direction. Any increase in Y_{21} decreases transvers bending stiffness as shown in Fig. 11. As seen in transverse specimens in Fig. 11, increased transverse bonding length 1 (Y_{21}) results in a reduction of the inclined Sections (2 and 4 shown in Fig. 7b), so the second moment of area and transverse bending stiffness decrease.

4.3. Evaluation of minor rib angle (θ_1)

To evaluate the effect of minor rib angle (θ_I) on the bending stiffness, longitudinal UC length (L_I) was also changed to keep other dimensions constant (Table 5).

Due to a decreasing width of the unit cells as the minor rib angle is increased (as shown in the transverse specimens in Fig. 12), the curvature in the x-axis and, in turn, the additional deflection in the longitudinal direction are reduced. Therefore, the normalized transverse bending stiffness increases (Fig. 12). For longitudinal specimens, since increased minor rib angle leads to shortening of the inclined Sections (2 and 4) and increase in the moment of inertia as shown in Fig. 7a, the longitudinal bending stiffness must increase. However, as the minor rib angle is increased, the fiber direction in the longitudinal direction deviates more and, thus, a decrease in the longitudinal bending stiffness is noticed. Therefore, this trend is not very well defined, since shortening

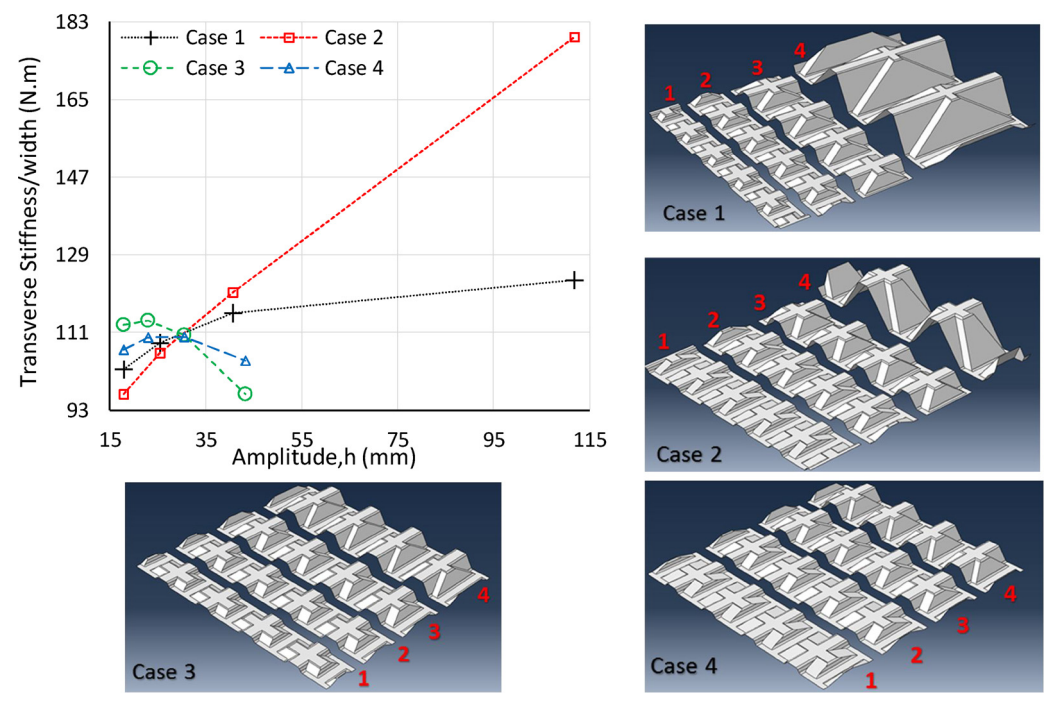


Fig. 8. Normalized bending stiffness and corresponding specimens for case 1-4 in transverse direction.

Table 4Corresponding cases and core parameters to evaluate transverse bonding lengths.

Case No.	Constant Parameters (mm)	Changing Parameters	Dimension o	Dimension of changing parameters for each UC (mm)		
			First UC	Second UC	Third UC	Fourth UC
5	$h = X_1 = Y_{21} = 25.4 L_1 = 135.32, \theta_1 = 25^{\circ}, t = 6.35$	L_2	108.65	134.05	286.45	565.85
		Y ₂₂	12.7	25.4	101.6	241.3
6	$h = X_1 = 25.4, L_1 = 135.32, \theta_1 = 25^{\circ}, t = 6.35$	L_2	81.22	113.73	144.21	286.45
		Y_{21}	12.19	20.32	27.94	63.5
		Y_{22}	12.19	20.32	27.94	63.5
7	$h = X_1 = 25.4$, $L_1 = 135.32$, $\theta_1 = 25^\circ$, $t = 6.35$, $Y_{22} = 12.19$	Y_{21}	12.19	28.96	41.66	112.78
		L_2	81.22	114.75	140.15	282.39

of the inclined sections and out-of-plane deviation of the fibers compete to increase and decrease the longitudinal bonding stiffness, respectively.

4.4. Evaluation of longitudinal bonding length (X_1)

Change in longitudinal bonding length, X_1 , as defined in Fig. 4 determines the area of adhesive bonding between the core and the outer plies, but also affects core's flexure behavior. Two cases were analyzed to understand the influence of X_1 (Table 6).

The result of the normalized bending stiffness in the longitudinal direction (Fig. 13) indicates that increasing the values of the changing parameters results in an upward trend for both cases. Since an increase in these parameters is followed by the shortening of the rib Sections (2 and 4 in Fig. 7a) and expansion of the horizontal Sections (1,3, and 5 in Fig. 7a), the bending stiffness is increased as a consequence of a rise in the average moment of inertia in the longitudinal direction.

Increasing the longitudinal bonding length, X_I , has a positive effect on transverse bonding stiffness of Case 9 due to shrinkage of inclined section which leads to an increase in moment of inertia (Fig. 14). However, a dual effect of rise and fall of the transverse bending stiffness in Case 10 is observed as shown in Fig. 14. This dual effect reveals that longitudinal bonding length (X_I) and longitudinal UC length (L_I) compete with each other to control the transverse bending stiffness. Initially, the effect of longitudinal bonding length is dominant as the average moment of inertia increases. However, beyond a critical point, longitudinal UC length becomes a predominant parameter and the transverse bending stiffness reduces. Increasing width resulting from increasing X_I (Case 10 in Fig. 14) leads to additional deflection in longitudinal direction when specimen is flexed in the transverse direction.

4.5. The effectiveness of core parameters

Before considering more cases, a review of the results obtained from these 10 cases merits discussion to understand the effectiveness of each parameter compared to others. Therefore, the percentage change in the normalized bending stiffness (as a consequence of change in variable parameters) are summarized in Table 7.

Cases one through four show the highest percentage changes in the longitudinal bending stiffness compared to those changes observed in other cases. Core amplitude, h, as a variable parameter in all these four cases has the most effective influence on the longitudinal bending stiffness. Increase in amplitude also has a positive increase, although not significantly, on the transverse bending stiffness ($\sim 12~\%$). Transverse bonding length 2 (Y_{22}) appears to be the most effective parameter to significantly alter the transverse bending stiffness (Cases 5 and 6). Y_{22} , however, reduces the longitudinal bending stiffness between 10-20~%. Since increased transverse bonding length 1 (Y_{21}) has a positive effect on the longitudinal bending stiffness as mentioned, Case 7 reveals that transverse UC length (L_1) has a negative influence, and its effect is more dominant than that of transverse bonding length 1 (Y_{21}).

Comparing the longitudinal bending stiffness of the first two cases reveals that, if amplitude is chosen as a variable parameter, increased minor rib angle (θ_1) is more effective than increased longitudinal UC length (L_1) in improving the longitudinal bending stiffness. However, when amplitude is held constant (as in Case 8), longitudinal UC length is more effective than minor rib angle. In Case 9, an increase in longitudinal bonding length (X_1) and minor rib angle (θ_1) results in an improvement of longitudinal and transverse bonding stiffness. Based on this fact and results of Case 8 and 10, it is evident that an increase in longitudinal UC length (L_1) has a positive effect on the longitudinal bending stiffness and a negative influence on the transverse bending stiffness; moreover, longitudinal UC length (L_1) is more effective than longitudinal bonding length (X_1) and minor rib angle (θ_1) .

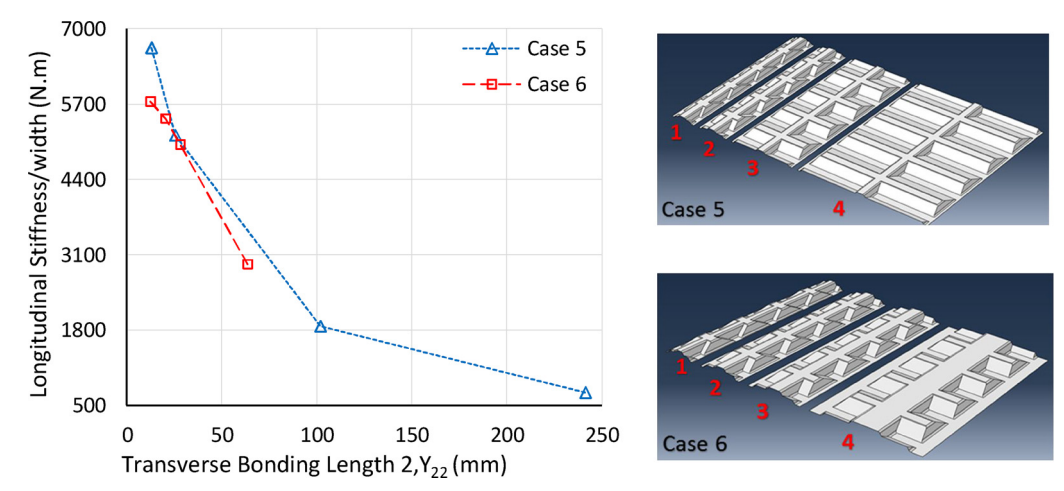


Fig. 9. Normalized bending stiffness and corresponding specimens for case 5 and 6 in longitudinal direction.

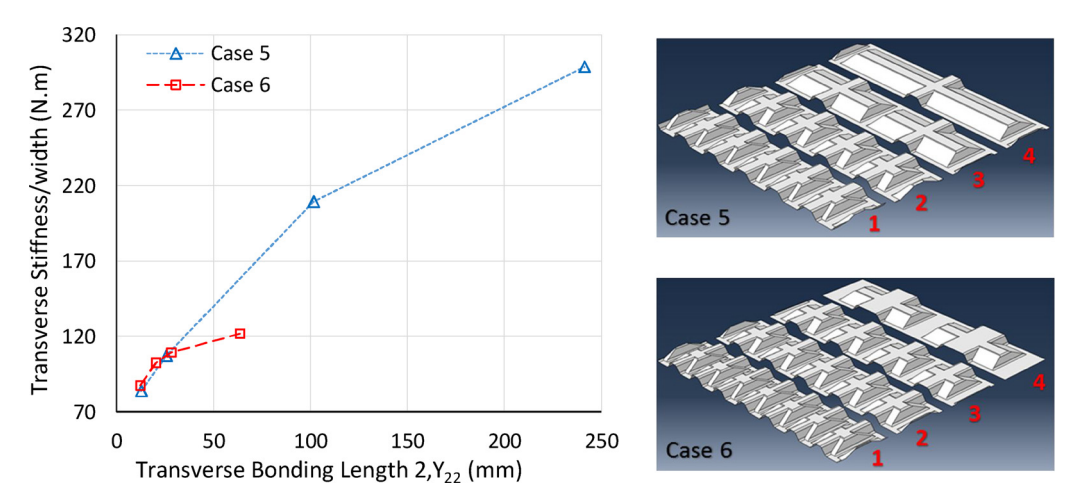


Fig. 10. Normalized bending stiffness and corresponding specimens for case 5 and 6 in transverse direction.

4.6. Evaluation of core wall thickness (t)

In Cases 11–13, the effect of core wall thickness on the longitudinal and transverse bending stiffnesses is investigated. Several cases that explore the interaction between wall thickness and other core parameters were developed, but only three cases are presented herein. Note that the span length of only transverse specimens was changed from 559 mm to 432 mm because of the limitation of the specimen configuration.

Since core wall thickness (t) is a normal parameter, any change in this parameter requires modifying a longitudinal and a transverse parameter as well. Three different cases as given in Table 8 are used to understand the effect of core wall thickness on the bending stiffness.

Any increase in wall thickness shows an increasing trend on both the longitudinal and transverse bending stiffnesses (Figs. 15 and 16). Increasing the wall thickness adds to the cross-section area, thus increasing the moment of inertia and bending stiffness of these specimens. As previously mentioned, any decrease in longitudinal and transverse UC length (L_1 and L_2) reduces longitudinal and transverse bending stiffness values. However, the results of Case 11 lead to the conclusion that thickness is much more effective than longitudinal and transverse UC length in altering the bending stiffness. Earlier analysis indicates that increase in transverse bonding length 2 (Y_{22}) has a negative effect on longitudinal bending stiffness. Results of Case 12 and Case 13 show that longitudinal bending stiffness increases even though transverse bonding length 2 (Y_{22}) also increases. These results re-confirm that thickness is more effective than transverse bonding length 2 to

change the longitudinal bending stiffness.

To determine the most effective case among the last three cases, percentage changes in normalized longitudinal and transverse bending stiffness were examined (Table 9). Comparison between these cases reveals that pairing core wall thickness with amplitude (h) and transverse bonding length 2 (Y_{22}) to change the core geometry results in a higher performance core.

5. Redesigning and validation

Based on the results obtained from the parametric study, the initial 3D core designed and fabricated by Voth [10] can be redesigned in order to achieve higher performance core. Certain limitations pertaining to the fabrication process must be considered within the design process. For instance, although the parametric study reveals that any increase in amplitude indicates improvement in the bending stiffness, there is an upper limit for amplitude due to limitation on how deep a wood strand preform can be formed. Since amplitude causes difference in the density of the horizontal and inclined sections of the core due to shear thinning or thickening, large amplitudes lead to weak sections as a consequence of low density. Additionally, as it is the intent in the future to use the 3D core in a mass timber panel, it is desirable to design the amplitude that is compatible with the thickness of solid layers, such as sawn or composite lumber [24]. Cavities introduced by the 3D core in mass timber panel can be then filled with insulation material to improve panel energy performance. Therefore, layers of lumber in a Cross Laminated Timber (CLT) can be replaced by layers of 3D core to

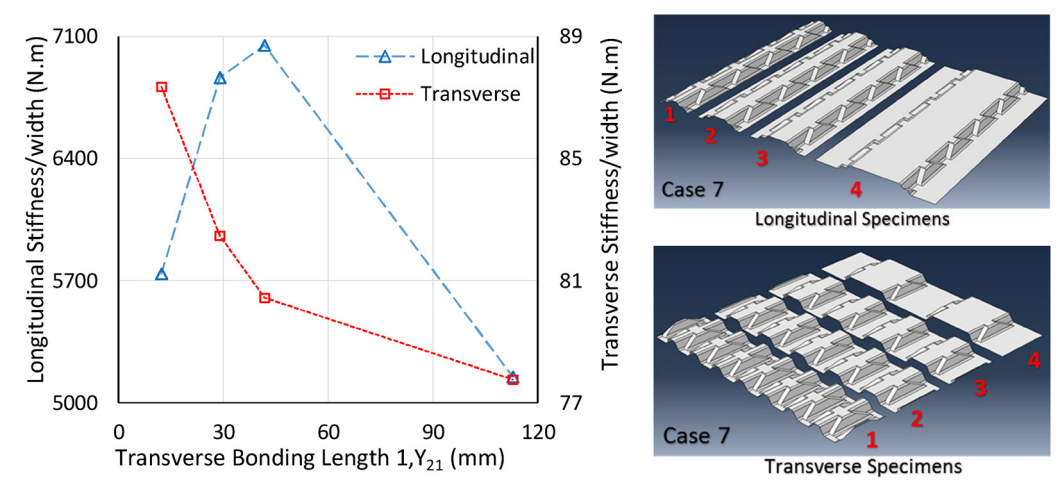


Fig. 11. Normalized bending stiffness and corresponding specimens for case 7 in the longitudinal and transverse directions.

Table 5Corresponding case and core parameters to evaluate minor rib angle.

Case No.	Constant Parameters (mm)	Changing Parameters	Dimension of	Dimension of changing parameters for each UC (mm)		
			First UC	Second UC	Third UC	Fourth UC
8	$h = X_1 = X_{21} = X_{22} = 25.4 L_2 = 134.05, t = 6.35$	$egin{array}{c} L_1 \ heta_1 \end{array}$	94.16 45°	113.23 33°	139.07 24°	267.99 10°

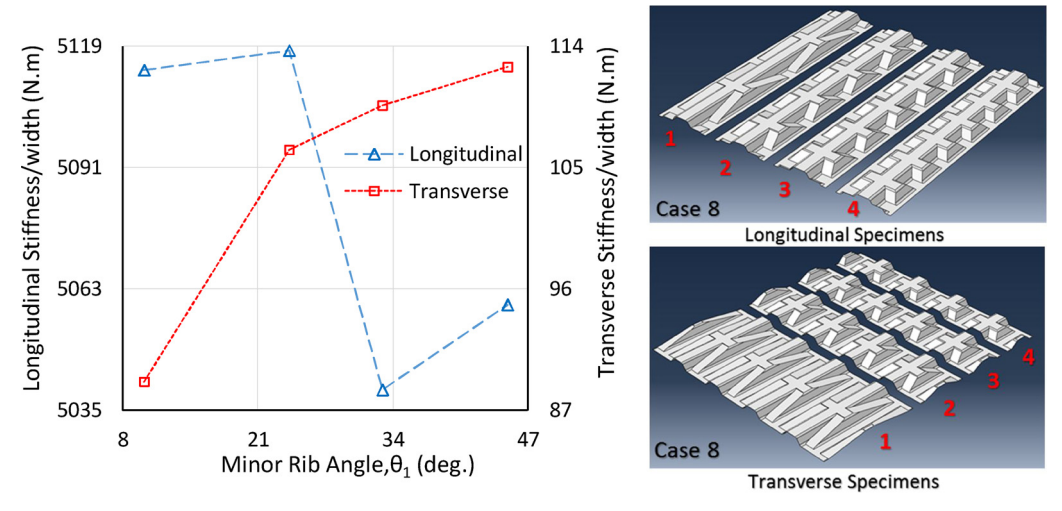


Fig. 12. Normalized bending stiffness and corresponding specimens for case 8 in the longitudinal and transverse directions.

Table 6Corresponding cases and core parameters to evaluate longitudinal bonding length.

Case No.	Constant Parameters (mm)	Changing Parameters	Dimension of changing parameters for each UC (mm)			
			First UC	Second UC	Third UC	Fourth UC
9	$h = X_{21} = X_{22} = 25.4$, $L_1 = 139.7$, $L_2 = 134.05$, $t = 6.35$	X_1	5.08	15.24	25.4	50.8
		Θ_1	16.61°	19.60°	23.84°	49.79°
10	$h = X_{21} = X_{22} = 25.4$, $L_2 = 134.05$, $\theta_1 = 30^\circ$, $t = 6.35$	X_1	12.19	20.32	38.1	101.6
		L_1	93.78	110.04	145.60	272.60

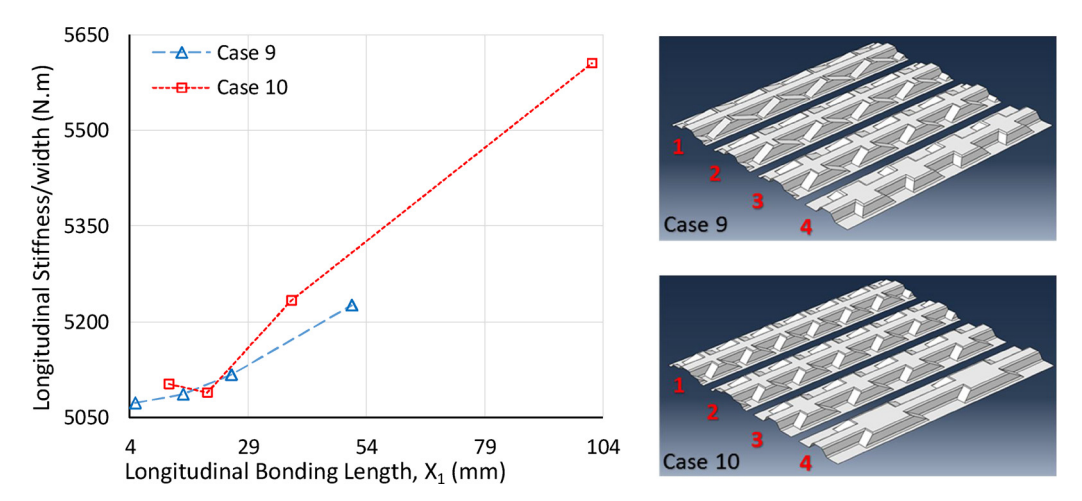


Fig. 13. Normalized bending stiffness and corresponding specimens for case 9 and 10 in longitudinal direction.

increase the energy performance. These practical applications were considered in the design process of the wood-strand core.

As the study indicated, any increase in minor rib angle would result in an increase in both the longitudinal and transverse bending stiffness. However, higher minor rib angle would lead to sharp edges that could potentially fracture the wood strands, and, thus, affecting the strength of the core panel negatively. Considering these limitations and the results of the parametric study, the core geometry was redesigned. The configuration and dimensions of one UC of the initial and redesigned cores are compared in Fig. 17.

The FE results of the four-point bending test conducted on the initial and redesigned core specimens are presented in Fig. 18. Span lengths in

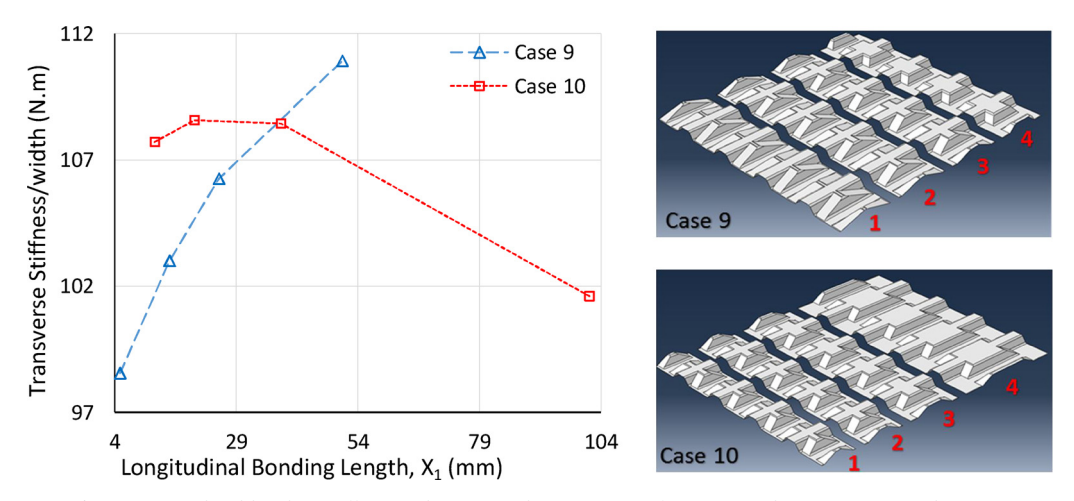


Fig. 14. Normalized bending stiffness and corresponding specimens for case 9 and 10 in transverse direction.

Table 7Percentage change in normalized bending stiffness of case 1–10 due to specific change in core parameters.

Case NO.	Changing Parameters	Initial Values (mm)	Altered Values (mm)	Change in Normalized Longitudinal Bending Stiffness	Change in Normalized Transverse Bending Stiffness
1	(h, L_1, L_2)	(25.4, 120.2, 134.1)	(40.6, 173, 154.6)	Increase 104 %	Increase 6.3 %
2	(h, θ_1, L_2)	(25.4, 24°, 134.1)	(40.6, 39°, 154.6)	Increase 118 %	Increase 13.2 %
3	(h, L_1, Y_{22})	(25.4, 120.1, 28.2)	(40.6, 173, 18)	Increase 178 %	Decrease 11.7 %
4	(h, θ_1, Y_{22})	(25.4, 23.7°, 28.2)	(40.6, 38.8°, 18)	Increase 218 %	Decrease 3.91 %
5	(Y_{22}, L_2)	(25.4, 134.1)	(38.1, 159.3)	Decrease 11 %	Increase 16 %
6	(Y_{22}, Y_{21}, L_2)	(19.1, 19.1, 108.5)	(38.1, 38.1, 174.5)	Decrease 19.7 %	Increase 12.8 %
7	(Y_{21}, L_2)	(22.9, 108.5)	(63.8, 184.7)	Decrease 2.9 %	Decrease 4.5 %
8	(θ_1, L_1)	(24°, 138.9)	(39°, 106.9)	Decrease 0.82 %	Increase 4.2 %
9	(X_1, θ_1)	(25.4, 24°)	(40.1, 39°)	Increase 1.24 %	Increase 2.44 %
10	(X_1, L_1)	(25.4, 120.1)	(40.1, 149.6)	Increase 2.24 %	Decrease 0.17 %

Table 8
Corresponding cases and core parameters to evaluate wall thickness (t).

Case No.	Constant Parameters (mm)	Changing Parameters	Dimension of changing parameters for each UC (mm)			
			First UC	Second UC	Third UC	Fourth UC
11	$h = 50.8, \theta_1 = 40^\circ, X_1 = 38.1, Y_{21} = 33.02, Y_{22} = 41.28$	t	3.18	6.35	9.53	12.7
· · · · · · · · · · · · · · · · · · ·	L_1	204.04	194.17	184.29	174.41	
		L_2	225.67	218.01	210.35	202.69
12	$L_1 = 194.17, L_2 = 218.01, \theta_1 = 40^{\circ}, X_1 = 38.1, Y_{21} = 33.02$	t	3.18	6.35	9.53	12.7
		h	46.65	50.8	54.95	59.09
		Y ₂₂	40.24	41.28	42.31	43.34
13	$h = 50.8$, $L_1 = 194.17$, $L_2 = 218.01$, $\theta_1 = 40^\circ$, $Y_{21} = 33.02$	t	3.18	6.35	9.53	12.7
	X_1	33.16	38.1	43.04	47.98	
		Y ₂₂	37.44	41.28	45.11	48.94

bending were 559 mm and 432 mm for longitudinal and transverse specimens, respectively. Based on the results obtained from the FE model and using Eq. (1), the normalized bending stiffnesses of the initial and redesigned core panels were computed. The redesigned core is 43 % and 126 % stiffer compared to the initial one in the longitudinal and transverse directions, respectively.

To fabricate core panels with the new geometry, a redesigned aluminum mold was manufactured (Fig. 19) and used to hot-press wood strand panels with biaxial corrugated geometry. Longitudinal and transverse core specimens of the redesigned core were tested and evaluated under four-point bending. Comparison of the experimental results (Fig. 18) show that the bending stiffness of the redesigned core is 59 % and 203 % greater than the initial one, in the longitudinal and transverse directions, respectively. In other words, the experimental results exceed the FE expectation, and the FE model errs on the side of

being conservative.

6. Conclusion

A systematic mechanic's approach was demonstrated to design wood-strand composite cores for use in wood composite sandwich panels for building envelope applications, and the approach was validated. A parametric analysis of a 3D wood strand core was conducted to study the influence of core geometry on the bending stiffness of the core and the sandwich panel. A verified FE model was utilized to perform a parametric study and understand the interdependency and influence of eight core geometric parameters. Core amplitude, width of the rib ridge, and core thickness are the most influential parameters that influence bending stiffness of the core and sandwich panels.

Based on the results of this parametric study and limitations of the

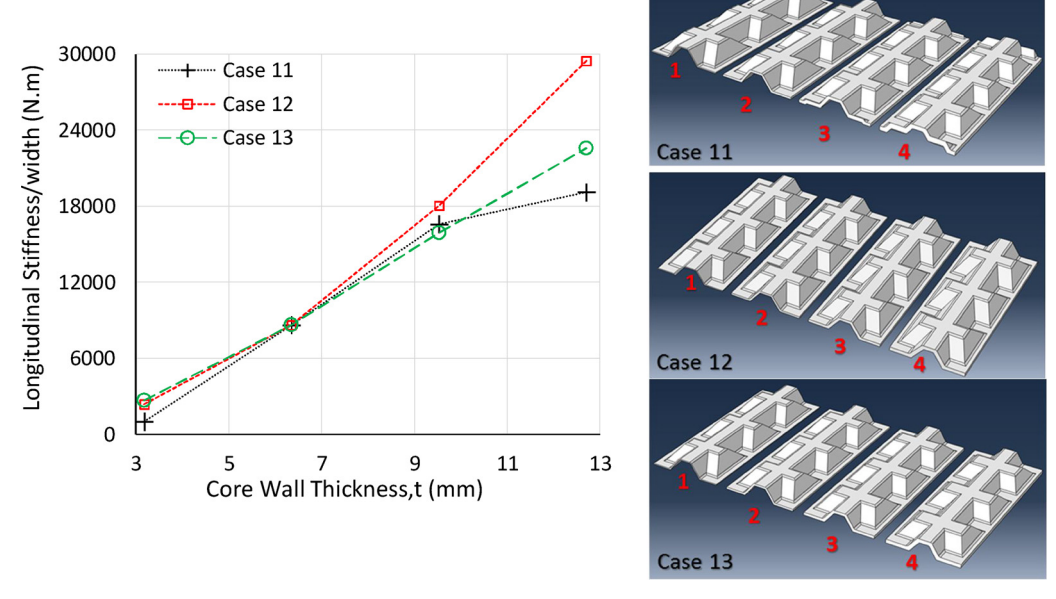


Fig. 15. Normalized bending stiffness and corresponding specimens for case 11-13 in longitudinal direction.

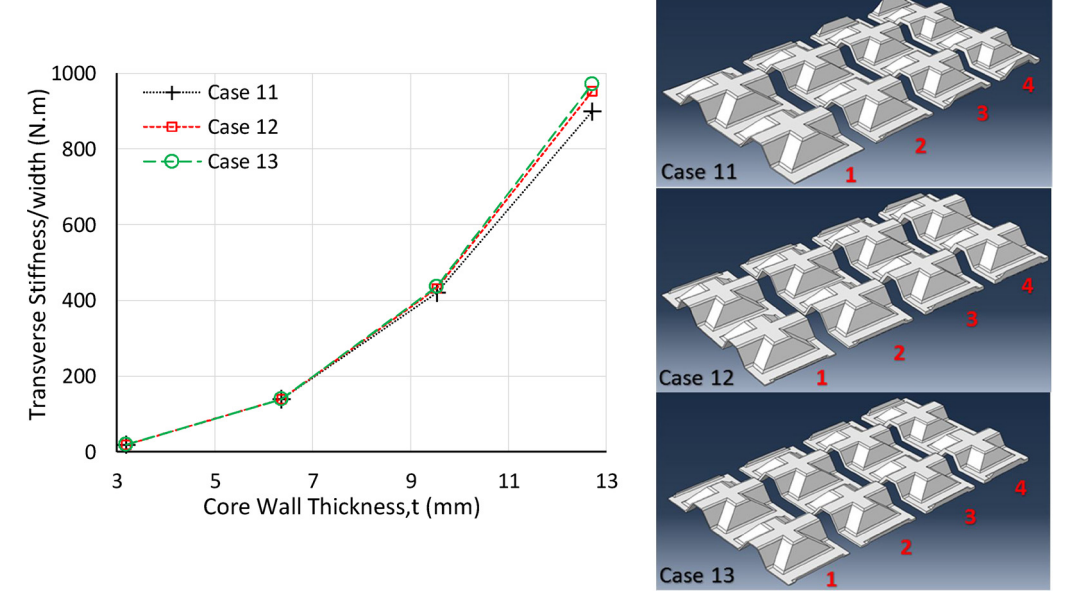


Fig. 16. Normalized bending stiffness and corresponding specimens for case 11-13 in Transverse direction.

Table 9 Percentage change in normalized bending stiffness of case 11–13.

Case NO.	Changing Parameters	Initial Values (mm)	Altered Values (mm)	Change in Normalized Longitudinal Bending Stiffness	Change in Normalized Transverse Bending Stiffness
11	(t,L_1,L_2)	(6.35, 194.1, 217.9)	(9.53, 184.2, 210.3)	Increase 92 %	Increase 203 %
12	(t, h, Y_{22})	(6.35, 50.8, 41.28)	(9.53, 54.86, 42.42)	Increase 109 %	Increase 211 %
13	(t, X_1, Y_{22})	(6.35, 38.1, 41.28)	(9.53, 43.18, 45.2)	Increase 84 %	Increase 214 %

fabrication process and future applications, a new mold was designed to hot press wood strand and to yield higher performance cores and sandwich panels. This high-performance core can be used to fabricate building envelopes of varying configurations to improve their structural and energy performance. Cavities within the sandwich panels resulting from inclusion of a single core or multiple cores can be filled with foam for improved sound and thermal insulation. Use of wood strands for

fabrication of these sandwich panels utilizes renewable feedstock, small diameter timber from hazardous fuel treatments, and leads to healthier forests.

CRediT authorship contribution statement

Mostafa Mohammadabadi: Methodology, Software, Validation,

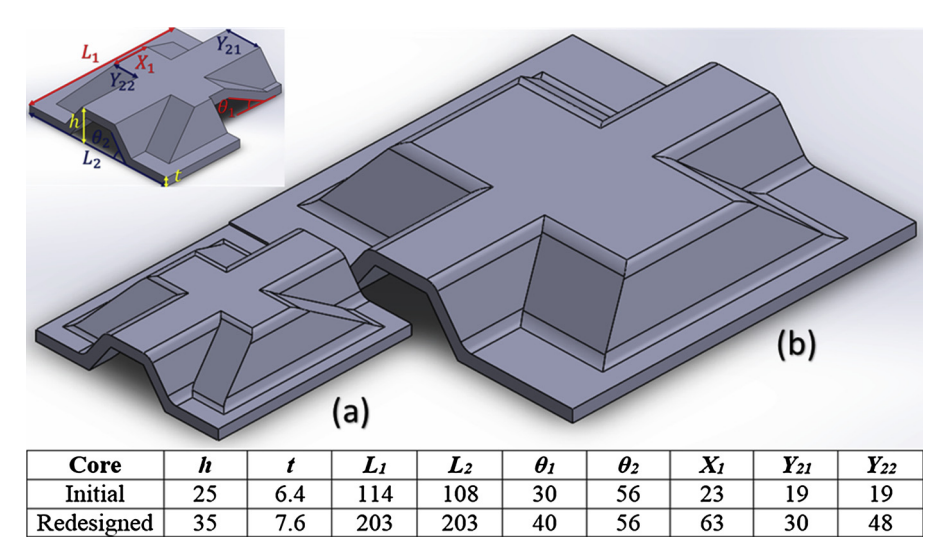


Fig. 17. Schematic view and dimension of (a) the initial core suggested by Voth [10] and (b) the redesigned core (Dimensions are in mm).

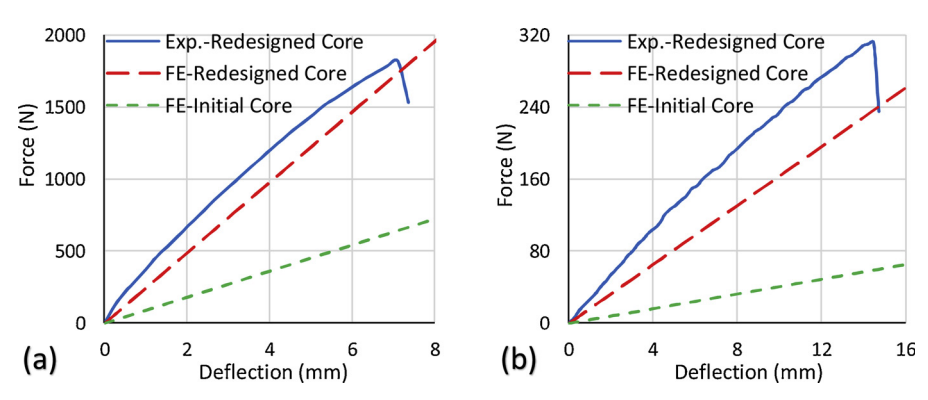


Fig. 18. Load-deflection curves for sandwich panel with initial and redesigned core in (a) longitudinal and (b) transverse directions.

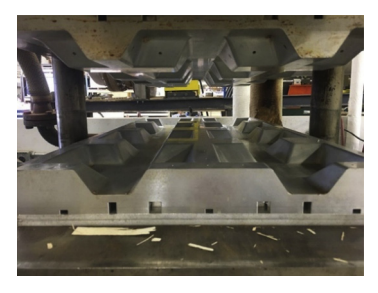


Fig. 19. New mold to fabricate the redesigned geometry.

Formal analysis, Investigation, Writing - original draft, Visualization. **Vikram Yadama:** Conceptualization, Funding acquisition, Project administration, Resources, Supervision, Data curation, Writing - review & editing.

Declaration of Competing Interest

The authors declare that they have no known competing financial interests or personal relationships that could have appeared to influence the work reported in this paper.

Acknowledgement

The authors would like to thank CMMI, National Science Foundation for funding this research, Grant # 1150316.

References

- L. He, Y.S. Cheng, J. Liu, Precise bending stress analysis of corrugated-core, honeycomb-core and X-core sandwich panels, Compos. Struct. 94 (April 5) (2012) 1656–1668.
- [2] S. Rao, R. Das, D. Bhattacharyya, Investigation of bond strength and energy absorption capabilities in recyclable sandwich panels, Compos. Part A Appl. Sci. Manuf. 45 (February) (2013) 6–13.
- [3] H.N. Spelter, D.B. McKeever, I. Durbak, Review of wood-based panel sector in United States and Canada, General technical report FPL; GTR-99) 99 (1997) 45 p ill.; 28 cm..
- [4] K.J. Fridley, Wood and wood-based materials: current status and future of a structural material, J. Mater. Civ. Eng. 14 (April 2) (2002) 91–96.
- [5] M. Mohamed, R. Hussein, A. Abutunis, Z. Huo, K. Chandrashekhara, L.H. Sneed, Manufacturing and evaluation of polyurethane composite structural insulated panels, J. Sandw. Struct. Mater. 18 (November 6) (2016) 769–789.
- [6] A. Kavianiboroujeni, A. Cloutier, D. Rodrigue, Mechanical characterization of asymmetric high density polyethylene/hemp composite sandwich panels with and without a foam core, J. Sandw. Struct. Mater. 17 (November 6) (2015) 748–765.
- [7] J.F. Hunt, J.E. Winandy, 3D engineered fiberboard: a new structural building product, InProceedings of the Sixth Panel Products Symposium, 2002 October 1-11, Llandudno, Wales, UK. Bangor, Gwynedd, UK: The BioComposites Centre, UWB, 2002, 2002 Pages 106-117.
- [8] S. Banerjee, D. Bhattacharyya, Optimal design of sandwich panels made of wood veneer hollow cores, Compos. Sci. Technol. 71 (February 4) (2011) 425–432.
- [9] D. Way, A. Sinha, F.A. Kamke, J.S. Fujii, Evaluation of a wood-strand molded core sandwich panel, J. Mater. Civ. Eng. 28 (March 9) (2016) 04016074.
- [10] C.R. Voth, Lightweight Sandwich Panels Using Small-diameter Timber Woodstrands and Recycled Newsprint Cores Doctoral Dissertation, Washington State University, 2020.
- [11] M. Mohammadabadi, V. Yadama, L. Yao, D. Bhattacharyya, Low-velocity impact response of wood-strand sandwich panels and their components, Holzforschung 72 (July 8) (2018) 681–689.
- [12] C. Voth, N. White, V. Yadama, W. Cofer, Design and evaluation of thin-walled hollow-core wood-strand sandwich panels, J. Renew. Mater. 3 (August 3) (2015) 234–243.
- [13] M. Mohammadabadi, V. Yadama, J. Geng, Creep behavior of 3D core wood-strand

- sandwich panels, Holzforschung 72 (June 6) (2018) 513-519.
- [14] T.M. Nordstrand, Parametric study of the post-buckling strength of structural core sandwich panels, Compos. Struct. 30 (January 4) (1995) 441–451.
- [15] J. Liu, Z. Wang, D. Hui, Blast resistance and parametric study of sandwich structure consisting of honeycomb core filled with circular metallic tubes, Compos. Part B Eng. 145 (July) (2018) 261–269.
- [16] A. Ermakova, I. Dayyani, Shape optimisation of composite corrugated morphing skins, Compos. Part B Eng. 115 (April) (2017) 87–101.
- [17] D. Bilston, G. Rathnaweera, D. Ruan, M. Hajj, Y. Durandet, Parametric study of the bending properties of lightweight tubular metal/polymer foam hybrid structures, Compos. Part B Eng. 105 (November) (2016) 101–110.
- [18] J.F. Hunt, 3D engineered fiberboard: finite element analysis of a new building product, In2004 International ANSYS Conference, Pittsburg, PA, May 24-26, 2004 [CD-ROM]. [Sl: sn, 2004]: 20 pages 2004.
- [19] F.A. Kamke, Physics of hot pressing, Proceedings of Fundamentals of Composite

- Processing, General Technical Report FPL-149, USDA Forest Service, Forest Products Laboratory, Madison, Wisconsin, 2004, pp. 3–18.
- [20] Mostafa Mohammadabadi, Vikram Yadama, Lloyd Smith, An analytical model for wood composite sandwich beams with a biaxial corrugated core under bending, Compos. Struct. 228 (November) (2019) 111316.
- [21] ASTM D 7249/D7249 M-06. Standard Test Method for Facing Properties of Sandwich Constructions by Long Beam Flexure, ASTM, West Conshohocken, PA, 2020.
- [22] A. Laulusa, O.A. Bauchau, J.Y. Choi, V.B. Tan, L. Li, Evaluation of some shear deformable shell elements, Int. J. Solids Struct. 43 (August 17) (2006) 5033–5054.
- [23] V. Yadama, M.P. Wolcott, L.V. Smith, Elastic properties of wood-strand composites with undulating strands, Compos. Part A Appl. Sci. Manuf. 37 (March 3) (2006) 385–392.
- [24] E. Karacabeyli, B. Douglas, CLT Handbook: Cross-laminated Timber, US Edition. FPInnovations, Pointe-Claire, QC, Canada, 2013.